519 **Supplementary materials.**

520

521 **Materials and Methods**

522

523 **Chimeric spike vaccine design and formulation**

524 Chimeric spike vaccines were designed with RBD and NTD swaps to increase coverage
525 of epidemic (SARS-CoV), pandemic (SARS-CoV-2), and high-risk pre-emergent bat CoVs (bat
526 SARS-like HKU3-1, and bat SARS-like RsSHC014). Chimeric and monovalent spike mRNA-
527 LNP vaccines were designed based on SARS-CoV-2 spike (S) protein sequence (Wuhan-Hu-1,
528 GenBank: MN908947.3), SARS-CoV (urbani GenBank: AY278741), bat SARS-like CoV
529 HKU3-1 (GenBank: DQ022305), and Bat SARS-like RsSHC014 (GenBank: KC881005).
530 Coding sequences of full-length SARS-CoV-2 furin knockout (RRAR furin cleavage site
531 abolished between amino acids 682-685), the four chimeric spikes, and the norovirus capsid
532 negative control were codon-optimized, synthesized and cloned into the mRNA production
533 plasmid mRNAs were encapsulated with LNP (*41*). Briefly, mRNAs were transcribed to contain
534 101 nucleotide-long poly(A) tails. mRNAs were modified with m1Ψ-5′-triphosphate (TriLink
535 #N-1081) instead of UTP and the *in vitro* transcribed mRNAs capped using the trinucleotide
536 cap1 analog, CleanCap (TriLink #N-7413). mRNA was purified by cellulose (Sigma-Aldrich #
537 11363-250G) purification. All mRNAs were analyzed by agarose gel electrophoresis and were
538 stored at -20°C. Cellulose-purified m1Ψ-containing RNAs were encapsulated in proprietary
539 LNPs containing adjuvant (Acuitas) using a self-assembly process as previously described
540 wherein an ethanolic lipid mixture of ionizable cationic lipid, phosphatidylcholine, cholesterol
541 and polyethylene glycol-lipid was rapidly mixed with an aqueous solution containing mRNA at

acidic pH. The RNA-loaded particles were characterized and subsequently stored at -80°C at a concentration of 1 mg/ml. The mean hydrodynamic diameter of these mRNA-LNP was ~80 nm with a polydispersity index of 0.02-0.06 and an encapsulation efficiency of ~95%.

Animals, immunizations, and challenge viruses

Eleven-month-old female BALB/c mice were purchased from Envigo (#047) and were used for all experiments. The study was carried out in accordance with the recommendations for care and use of animals by the Office of Laboratory Animal Welfare (OLAW), National Institutes of Health and the Institutional Animal Care and Use Committee (IACUC) of University of North Carolina (UNC permit no. A-3410-01). mRNA-LNP vaccines were kept frozen until right before the vaccination. Mice were immunized with a total 1μg in the prime and boost. Briefly, chimeric vaccines were mixed at 1:1 ratio for a total of 1μg when more than one chimeric spike was used or 1μg of a single spike diluted in sterile 1XPBS in a 50μl volume and were given 25μl intramuscularly in each hind leg. Prime and boost immunizations were given three weeks apart. Three weeks post boost, mice were bled, sera was collected for analysis, and mice were moved into the BSL3 facility for challenge experiments. Animals were housed in groups of five and fed standard chow diets. Virus inoculations were performed under anesthesia and all efforts were made to minimize animal suffering. All mice were anesthetized and infected intranasally with 1×10^4 PFU/ml of SARS-CoV MA15, 1×10^4 PFU/ml of SARS-CoV-2 MA10, 1×10^4 PFU/ml RsSHC014, 1×10^4 PFU/ml RsSHC014-MA15, 1×10^5 PFU/ml WIV-1, and 1×10^4 PFU/ml SARS-CoV-2 B.1.351-MA10 which have been described previously (*8*, *42*, *43*). Mice were weighted daily and monitored for signs of clinical disease. Each challenge virus challenge experiment encompassed 50 mice with 10 mice per vaccine group to obtain statistical

565 power. Mouse vaccinations and challenge experiments were independently repeated twice to
566 ensure reproducibility.
567
568 **Measurement of mouse CoV spike binding antibodies by ELISA**
569 Mouse serum samples from pre-immunization (pre-prime), 2 weeks post prime (pre-
570 boost), and 3 weeks post boost were tested. A binding ELISA panel that included SARS-CoV
571 spike Protein DeltaTM, SARS-CoV-2 (2019-nCoV) spike Protein (S1+S2 ECD, His tag),
572 MERS-CoV, Coronavirus spike S1+S2 (Baculovirus-Insect Cells, His), HKU1 (isolate N5) spike
573 Protein (S1+S2 ECD, His Tag), OC43 spike Protein (S1+S2 ECD, His Tag), 229E spike Protein
574 (S1+S2 ECD, His tag) Human coronavirus (HCoV-NL63) spike Protein (S1+S2 ECD, His Tag),
575 Pangolin CoV_GXP4L_spikeEcto2P_3C8HtS2/293F, bat CoV
576 RsSHC014_spikeEcto2P_3C8HtS2/293F, RaTG13_spikeEcto2P_3C8HtS2/293F, and bat CoV
577 HKU3-1 spike were tested. Indirect binding ELISAs were conducted in 384 well ELISA plates
578 (Costar #3700) coated with 2µg/ml antigen in 0.1M sodium bicarbonate overnight at 4°C,
579 washed and blocked with assay diluent (1XPBS containing 4% (w/v) whey protein/ 15% Normal
580 Goat Serum/ 0.5% Tween-20/ 0.05% Sodium Azide). Serum samples were incubated for 60
581 minutes in three-fold serial dilutions beginning at 1:30 followed by washing with PBS/0.1%
582 Tween-20. HRP conjugated goat anti-mouse IgG secondary antibody (SouthernBiotech 1030-05)
583 was diluted to 1:10,000 in assay diluent without azide, incubated at for 1 hour at room
584 temperature, washed and detected with 20µl SureBlue Reserve (KPL 53-00-03) for 15 minutes.
585 Reactions were stopped via the addition of 20µl HCL stop solution. Plates were read at 450nm.
586 Area under the curve (AUC) measurements were determined from binding of serial dilutions.
587

588 **ACE2 blocking ELISAs.**

589 Plates were coated with 2μg/ml recombinant ACE2 protein, then washed and blocked
590 with 3% BSA in PBS. While assay plates blocked, and sera was diluted 1:25 in 1%BSA/0.05%
591 Tween-20. Then SARS-CoV-2 spike protein was mixed with equal volumes of each sample at a
592 final spike concentration equal to the EC_{50} at which it binds to ACE2. The mixture was allowed
593 to incubate at room temperature for 1 hour. Blocked assay plates were washed, and the serum-
594 spike mixture was added to the assay plates for a period of 1 hour at room temperature. Plates
595 were washed and Strep-Tactin HRP, (IBA GmbH, Cat# 2-1502-001) was added at a dilution of
596 1:5000 followed by TMB substrate. The extent to which antibodies were able to block the
597 binding of spike protein to ACE2 was determined by comparing the OD of antibody samples at
598 450nm to the OD of samples containing spike protein only with no antibody. The following
599 formula was used to calculate percent blocking (100-(OD sample/OD of spike only) *100).
600
601 **Measurement of neutralizing antibodies against live viruses**
602 Full-length SARS-CoV-2 Seattle, SARS-CoV-2 D614G, SARS-CoV-2 B.1.351, SARS-
603 CoV-2 B.1.1.7, SARS-CoV-2 mink, SARS-CoV, WIV-1, and RsSHC014 viruses were designed
604 to express nanoluciferase (nLuc) and were recovered via reverse genetics as described previously
605 (*29*). Virus titers were measured in Vero E6 USAMRIID cells, as defined by plaque forming
606 units (PFU) per ml, in a 6-well plate format in quadruplicate biological replicates for accuracy.
607 For the 96-well neutralization assay, Vero E6 USAMRID cells were plated at 20,000 cells per
608 well the day prior in clear bottom black walled plates. Cells were inspected to ensure confluency
609 on the day of assay. Serum samples were tested at a starting dilution of 1:20 and were serially
610 diluted 3-fold up to nine dilution spots. Serially diluted serum samples were mixed in equal

volume with diluted virus. Antibody-virus and virus only mixtures were then incubated at 37°C with 5% CO_2 for one hour. Following incubation, serially diluted sera and virus only controls were added in duplicate to the cells at 75 PFU at 37°C with 5% CO_2. After 24 hours, cells were lysed, and luciferase activity was measured via Nano-Glo Luciferase Assay System (Promega) according to the manufacturer specifications. Luminescence was measured by a Spectramax M3 plate reader (Molecular Devices, San Jose, CA). Virus neutralization titers were defined as the sample dilution at which a 50% reduction in RLU was observed relative to the average of the virus control wells.

Eosinophilic lung infiltrates staining

To detect eosinophils, chromogenic immunohistochemistry (IHC) was performed on paraffin-embedded lung tissues that were sectioned at 4 microns. Lung tissues from vaccine groups 1-5 were analyzed for lung eosinophilic infiltration. N=8-10 lung tissues per group were analyzed. This IHC was carried out using the Leica Bond III Autostainer system. Slides were dewaxed in Bond Dewax solution (AR9222) and hydrated in Bond Wash solution (AR9590). Heat induced antigen retrieval was performed for 20 min at 100ºC in Bond-Epitope Retrieval solution 2, pH-9.0 (AR9640). After pretreatment, slides were incubated with an Eosinophil Peroxidase antibody (PA5-62200, Invitrogen) at 1:1,000 for 1h followed with Novolink Polymer (RE7260-K) secondary. Antibody detection with 3,3'-diaminobenzidine (DAB) was performed using the Bond Intense R detection system (DS9263). Stained slides were dehydrated and coverslipped with Cytoseal 60 (8310-4, Thermo Fisher Scientific). Two positive controls (one with high and another with low eosinophil reactivity) and a negative control (no primary antibody) were included in all staining runs.

634

635 **Lung pathology scoring**

636 Acute lung injury was quantified via two separate lung pathology scoring scales: Matute-
637 Bello and Diffuse Alveolar Damage (DAD) scoring systems. Analyses and scoring were
638 performed by a board vertified veterinary pathologist who was blinded to the treatment groups as
639 described previously (*30*). Lung pathology slides were read and scored at 600X total
640 magnification.

641 The lung injury scoring system used is from the American Thoracic Society (Matute-
642 Bello) in order to help quantitate histological features of ALI observed in mouse models to relate
643 this injury to human settings. In a blinded manner, three random fields of lung tissue were
644 chosen and scored for the following: (A) neutrophils in the alveolar space (none = 0, 1–5 cells =
645 1, > 5 cells = 2), (B) neutrophils in the interstitial septa (none = 0, 1–5 cells = 1, > 5 cells = 2),
646 (C) hyaline membranes (none = 0, one membrane = 1, > 1 membrane = 2), (D) Proteinaceous
647 debris in air spaces (none = 0, one instance = 1, > 1 instance = 2), (E) alveolar septal thickening
648 (< 2x mock thickness = 0, 2–4x mock thickness = 1, > 4x mock thickness = 2). To obtain a lung
649 injury score per field, A–E scores were put into the following formula score = [(20x A) + (14 x
650 B) + (7 x C) + (7 x D) + (2 x E)]/100. This formula contains multipliers that assign varying
651 levels of importance for each phenotype of the disease state. The scores for the three fields per
652 mouse were averaged to obtain a final score ranging from 0 to and including 1.
653 The second histology scoring scale to quantify acute lung injury was adopted from a lung
654 pathology scoring system from lung RSV infection in mice (*31*). This lung histology scoring
655 scale measures diffuse alveolar damage (DAD). Similar to the implementation of the ATS
656 histology scoring scale, three random fields of lung tissue were scored for the following in a

blinded manner: 1= absence of cellular sloughing and necrosis, 2=Uncommon solitary cell sloughing and necrosis (1–2 foci/field), 3=multifocal (3+foci) cellular sloughing and necrosis with uncommon septal wall hyalinization, or 4=multifocal (>75% of field) cellular sloughing and necrosis with common and/or prominent hyaline membranes. The scores for the three fields per mouse were averaged to get a final DAD score per mouse. The microscope images were generated using an Olympus Bx43 light microscope and CellSense Entry v3.1 software.

Measurement of lung cytokines

Lung tissue was homogenized, spun down at 13,000g, and supernantant was used to measure lung cytokines using Mouse Cytokine 23-plex Assay (BioRad). Briefly, 50µl of lung homogenate supernatant was added to each well and the protocol was followed according to the manufacturer specifications. Plates were read using a MAGPIX multiplex reader (Luminex Corporation).

Biocontainment and biosafety

Studies were approved by the UNC Institutional Biosafety Committee approved by animal and experimental protocols in the Baric laboratory. All work described here was performed with approved standard operating procedures for SARS-CoV-2 in a biosafety level 3 (BSL-3) facility conforming to requirements recommended in the Microbiological and Biomedical Laboratories, by the U.S. Department of Health and Human Service, the U.S. Public Health Service, and the U.S. Center for Disease Control and Prevention (CDC), and the National Institutes of Health (NIH).

Statistics

All statistical analyses were performed using GraphPad Prism 9. Statistical tests used in each figure are denoted in the corresponding figure legend.

Figure S1. Chimeric and wild type spike Sarbecovirus constructs.

(**A**) Mouse vaccination strategy using mRNA-LNPs: group 1 received chimeric spike 1, 2, 3, and 4 as the prime and boost, group 2 received chimeric spike 1, 2 as the prime and chimeric spikes 3 and 4 as the boost, group 3 received chimeric spike 4 as the prime and boost, group 4 received SARS-CoV-2 furin KO prime and boost, and group 5 received a norovirus capsid prime and boost. Different vaccine groups were separately challenged with 1) SARS-CoV MA15, 2) SARS-CoV-2 MA10, 3) RsSHC014 full-length virus, 4) RsSHC014-MA15, 5) WIV-1, and 6) SARS-CoV-2 B.1.351 MA10. (**B**) Protein expression of chimeric spikes, SARS-CoV-2 furin KO, and norovirus mRNA vaccines. The extra band between 100-150 kDa corresponds to S1. GAPDH was used as the loading control. (**C**) Nanoluciferase expression of RsSHC014/SARS-CoV-2 chimeric spike live viruses.

Figure S2. Human common-cold CoV ELISA binding responses in chimeric and monovalent SARS-CoV-2 spike mRNA-LNP-vaccinated mice. Pre-immunization, post prime, and post boost binding to (**A**) HCoV-HKU1 spike, (**B**) HCoV-OC43 spike, (**C**) HCoV-229E spike, and (**D**) HCoV-NL63 spike. Statistical significance for the binding and blocking responses is reported from a Kruskal-Wallis test after Dunnett's multiple comparison correction. $^{*}p < 0.05$, $^{**}p < 0.01$, $^{***}p < 0.001$, and $^{****}p < 0.0001$.

Figure S3. Comparison of neutralizing antibody activity of CoV mRNA-LNP vaccines against Sarbecoviruses. (**A**) Group 1 neutralizing antibody responses against SARS-CoV-2, SARS-CoV, RsSHC014, and WIV-1 and (**B**) fold-change of SARS-CoV, RsSHC014, and WIV-1 neutralizing antibodies relative to SARS-CoV-2. (**C**) Group 2 neutralizing antibody responses

against SARS-CoV-2, SARS-CoV, RsSHC014, and WIV-1 and (**D**) fold-change of SARS-CoV, RsSHC014, and WIV-1 neutralizing antibodies relative to SARS-CoV-2. (**E**) Group 3 neutralizing antibody responses against SARS-CoV-2, SARS-CoV, RsSHC014, and WIV-1 and (**F**) fold-change of SARS-CoV, RsSHC014, and WIV-1 neutralizing antibodies relative to SARS-CoV-2. (**G**) Group 4 neutralizing antibody responses against SARS-CoV-2, SARS-CoV, RsSHC014, and WIV-1 and (**H**) fold-change of SARS-CoV, RsSHC014, and WIV-1 neutralizing antibodies relative to SARS-CoV-2.

Figure S4. *In vivo* protection against Bt-CoV challenge by chimeric spikes mRNA-vaccines. (**A**) Percent starting weight from the different vaccine groups of mice challenged with full-length RsSHC014. (**B**) RsSHC014 lung viral titers in mice from the distinct vaccine groups. (**C**) RsSHC014 nasal turbinate titers in mice from the different immunization groups. (**D**) Percent starting weight from the different vaccine groups of mice challenged with RsSHC014-MA15. (**E**) RsSHC014-MA15 lung viral titers in mice from the distinct vaccine groups. (**F**) RsSHC014-MA15 nasal turbinate titers in mice from the different immunization groups. Statistical significance is reported from a one-way ANOVA after Tukey's multiple comparison correction. $^{*}p < 0.05$, $^{**}p < 0.01$, $^{***}p < 0.001$, and $^{****}p < 0.0001$.

Figure S5. Survival analysis of immunized mice challenged with Sarbecoviruses. (**A**) Survival analysis at day 4 post infection from immunized mice infected with SARS-CoV MA15, (**B**) SARS-CoV-2 MA10, (**C**) Survival analysis at day 7 post infection from immunized mice infected with SARS-CoV-2 MA10, and (**D**) RsSHC014-MA15. Statistical significance is reported from a Mantel-Cox test.

Figure S6. Detection of eosinophilic infiltrates in SARS-CoV MA15 challenged mice. (**A**) Group 1: rare scattered individual eosinophils in the interstitium with some small perivascular cuffs that lack eosinophils. (**B**) Group 2: Bronchiolar cuffs of leukocytes with rare eosinophils. (**C**) Group 3: Hyperplastic bronchus-associated lymphoid tissue (BALT) with rare eosinophils. (**D**) Group 4: frequent perivascular cuffs that contain eosinophils. (**E**) Group 5: frequent eosinophils in perivascular cuffs.

Figure S7. Lung cytokine analysis in Sarbecovirus-challenged mice. CCL2, IL-1α, G-SCF, and CCL4 in (**A**) SARS-CoV-infected mice and in (**B**) SARS-CoV-2-infected mice. Statistical significance for the binding and blocking responses is reported from a Kruskal-Wallis test after Dunnett's multiple comparison correction. $^{*}p < 0.05$, $^{**}p < 0.01$, $^{***}p < 0.001$, and $^{****}p < 0.0001$.

Table S1: Amino acid sequences of chimeric spikes.

Figure S1

A

Immunization strategy and challenge viruses in the different vaccine groups.

Vaccination group	Day 0 prime	Day 21 boost	Day 55 post prime challenge viruses
Group 1	Chimera 1, 2, 3, 4	Chimera 1, 2, 3, 4	1) SARS-CoV MA15, 2) SARS-CoV-2 MA10 3) RsSHC014, 4) RsSHC014-MA15 5) WIV-1, 6) SARS-CoV-2 B.1.351-MA10
Group 2	Chimera 1, 2	Chimera 3, 4	1) SARS-CoV MA15, 2) SARS-CoV-2 MA10 3) RsSHC014, 4) RsSHC014-MA15 5) WIV-1, 6) SARS-CoV-2 B.1.351-MA10
Group 3	Chimera 4	Chimera 4	1) SARS-CoV MA15, 2) SARS-CoV-2 MA10 3) RsSHC014, 4) RsSHC014-MA15 5) WIV-1, 6) SARS-CoV-2 B.1.351-MA10
Group 4	SARS-CoV-2 furin knockout	SARS-CoV-2 furin knockout	1) SARS-CoV MA15, 2) SARS-CoV-2 MA10 3) RsSHC014, 4) RsSHC014-MA15 5) WIV-1, 6) SARS-CoV-2 B.1.351-MA10
Group 5	Norovirus capsid	Norovirus capsid	1) SARS-CoV MA15, 2) SARS-CoV-2 MA10 3) RsSHC014, 4) RsSHC014-MA15 5) WIV-1, 6) SARS-CoV-2 B.1.351-MA10

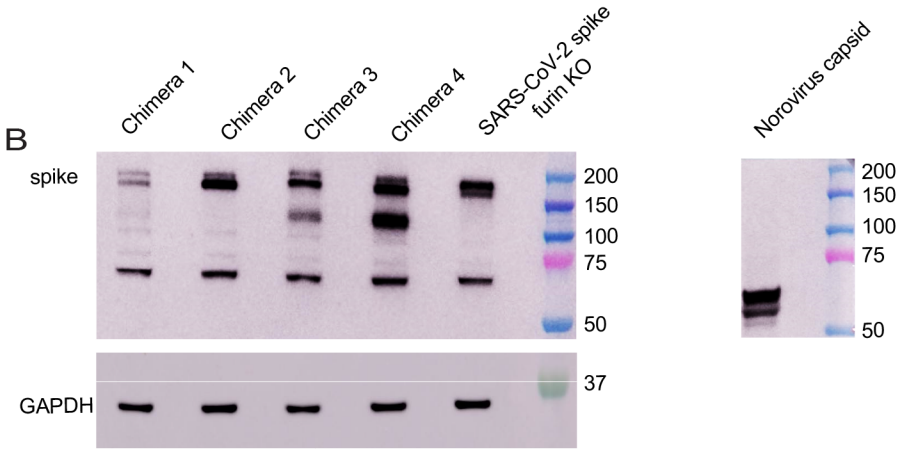

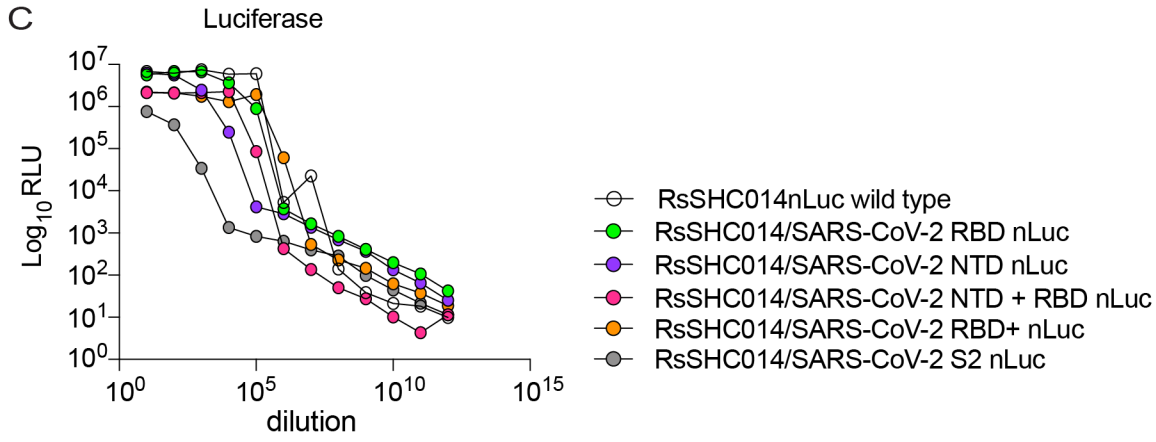

Figure S2

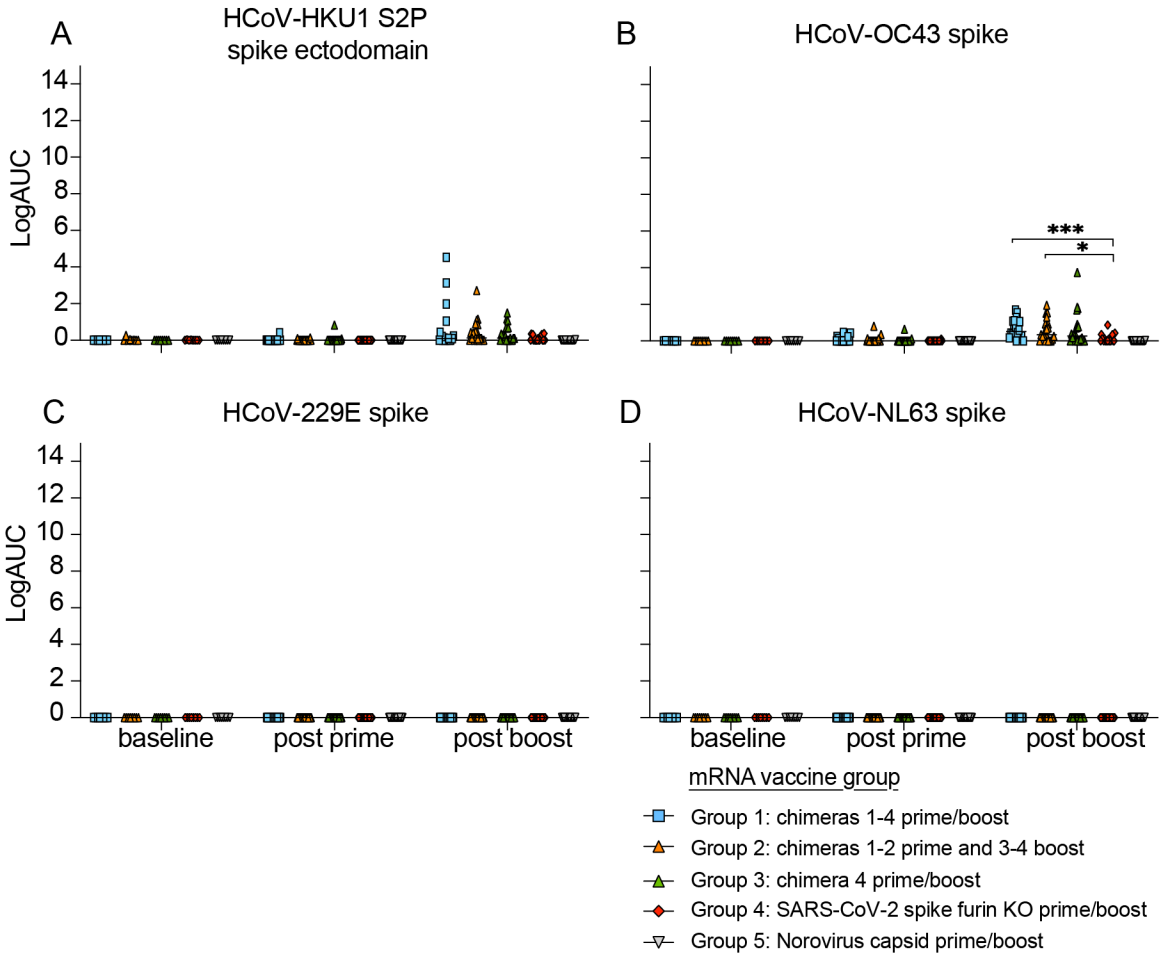

Figure S3

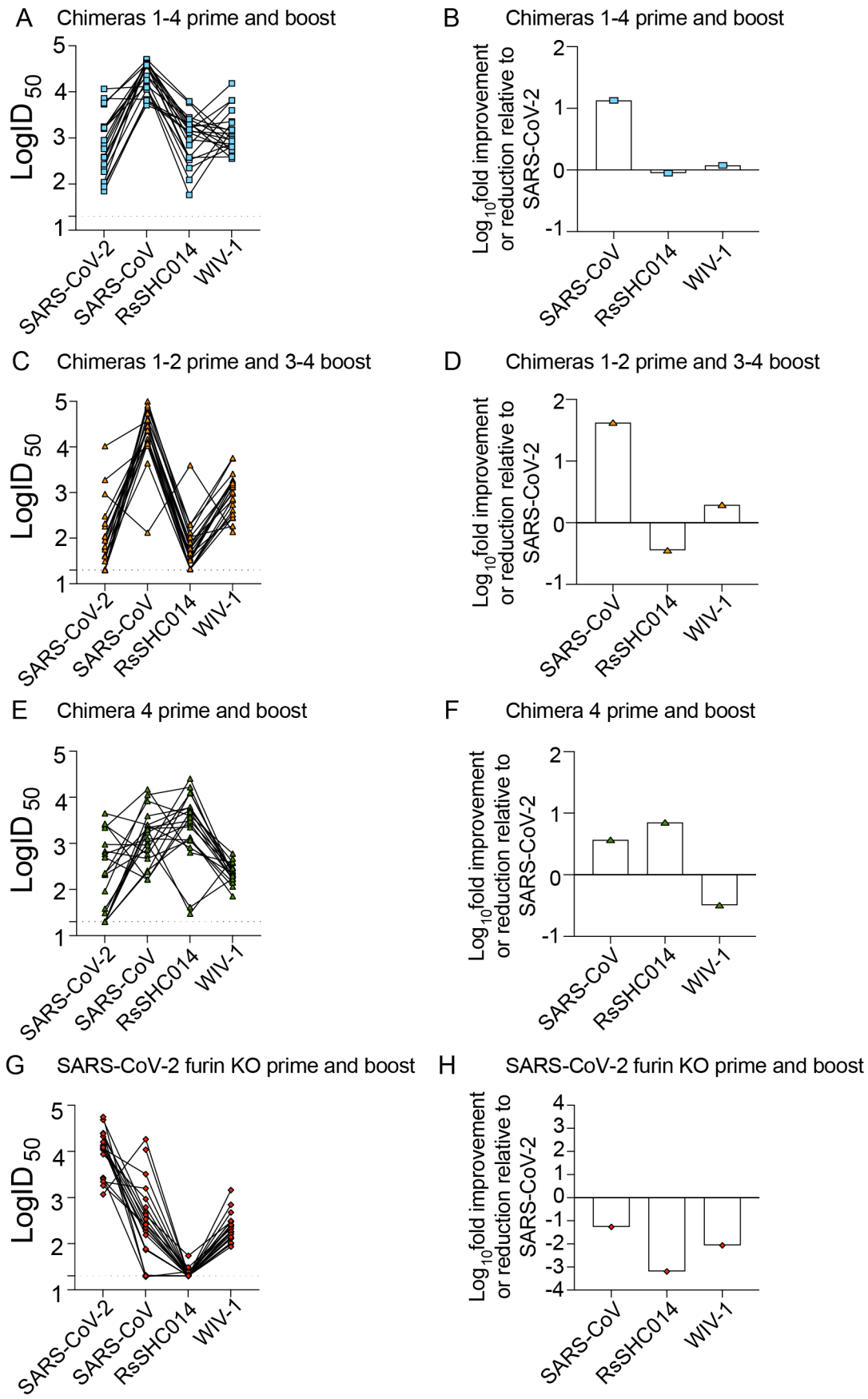

Figure S4

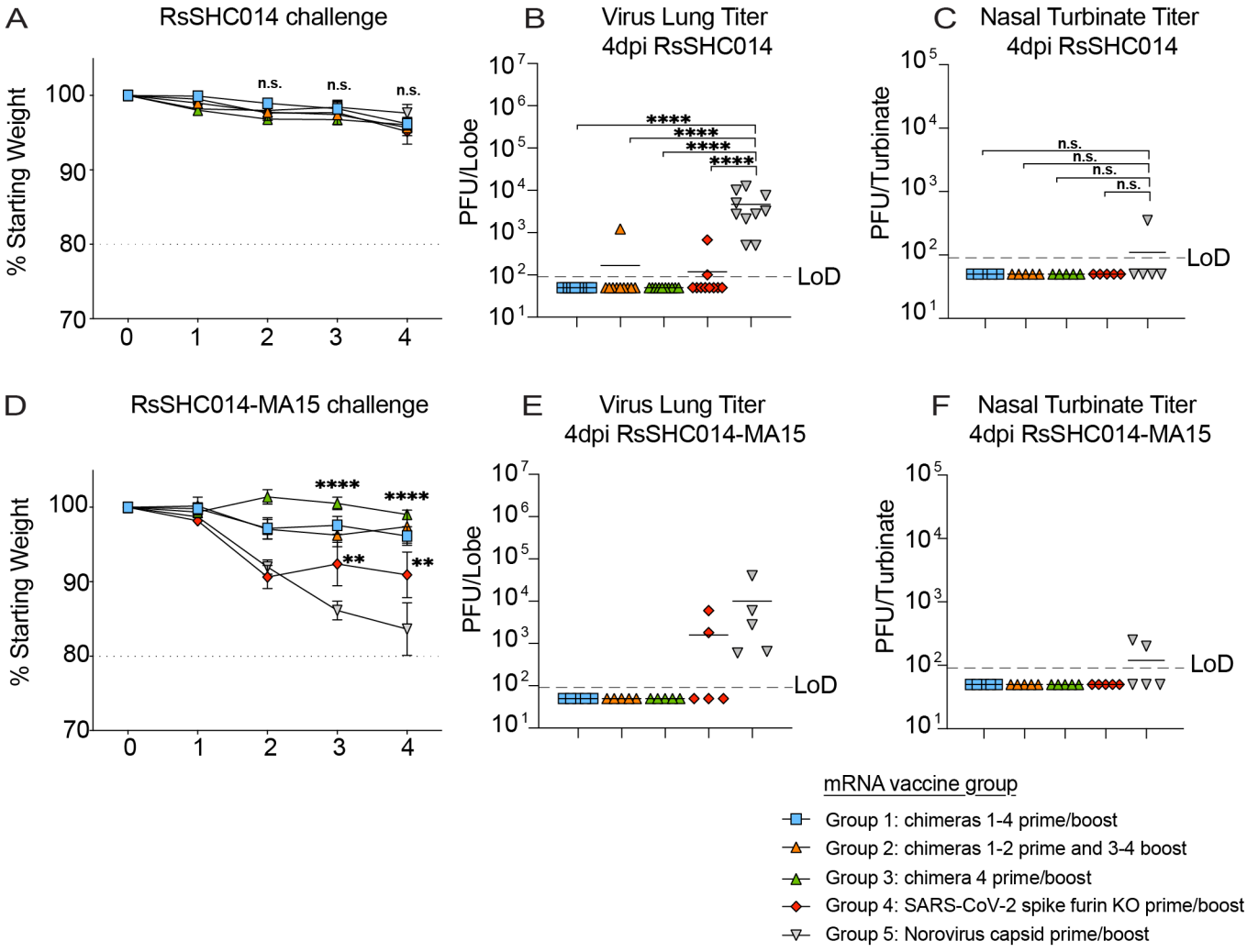

Figure S5

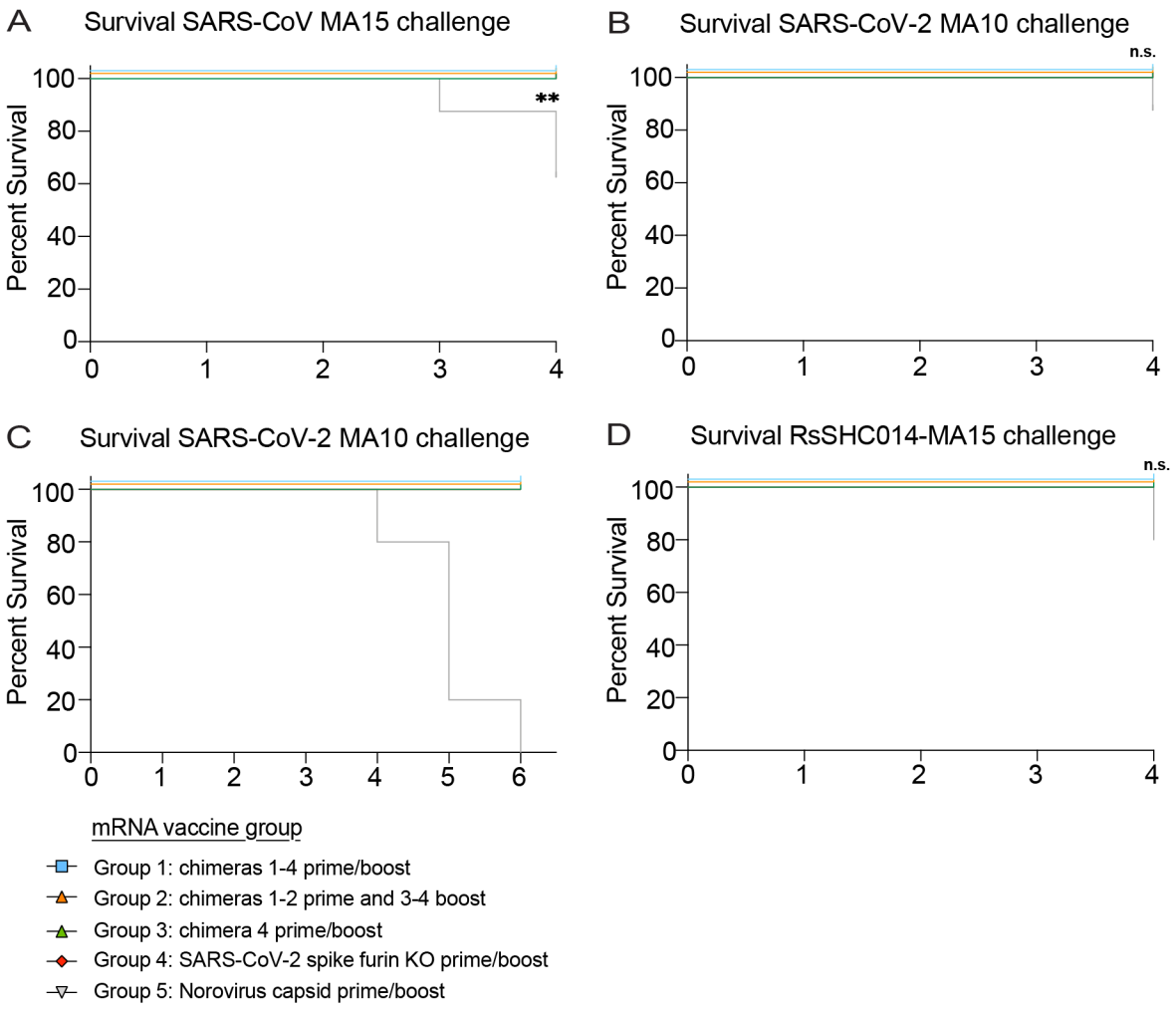

Figure S6

SARS-CoV challenge

A Group 1

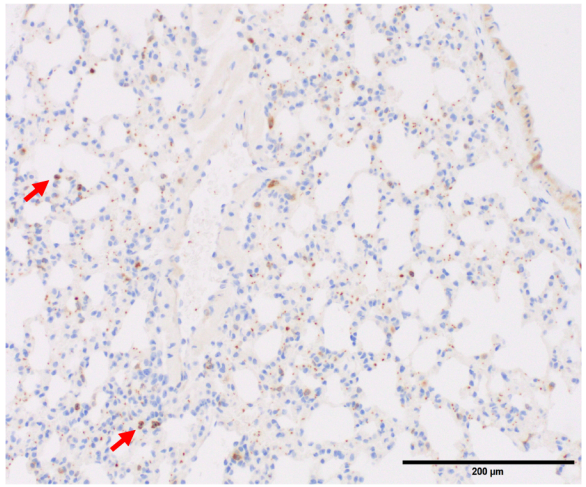

B Group 2

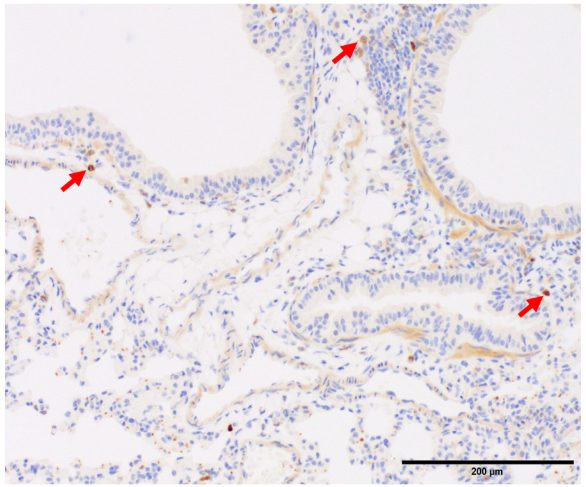

C Group 3

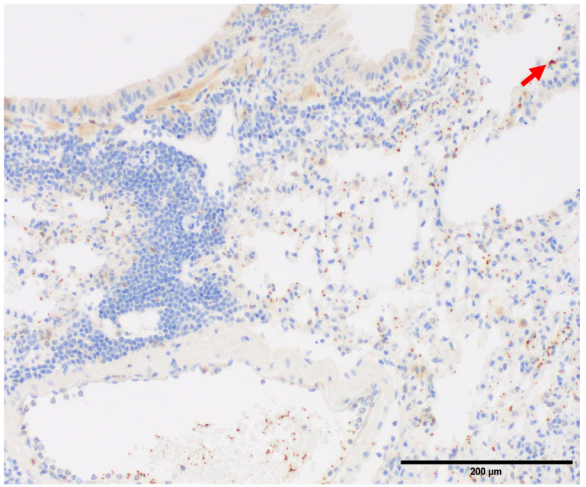

D Group 4

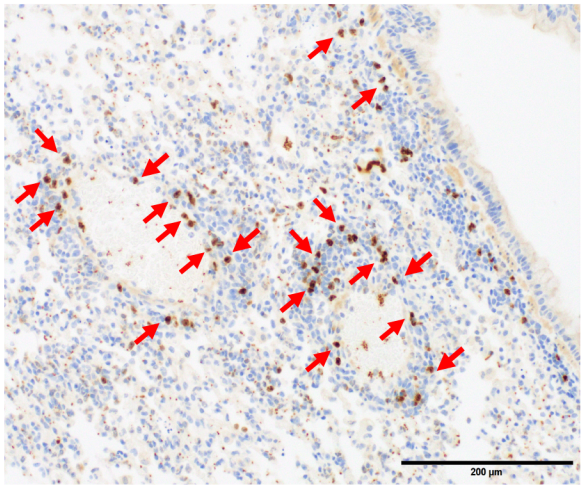

E Group 5

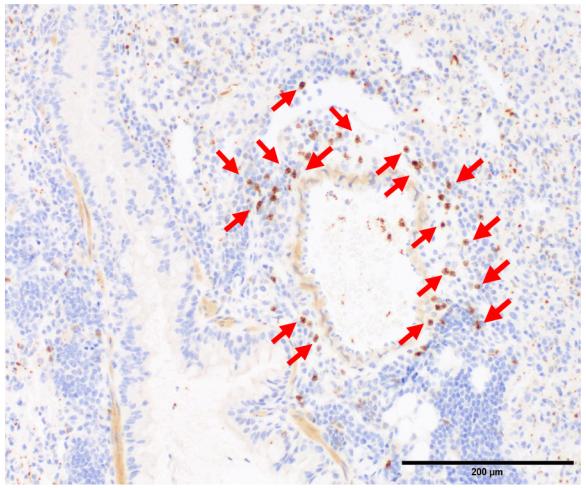

mRNA vaccine group

- Group 1: chimeras 1-4 prime/boost
- Group 2: chimeras 1-2 prime and 3-4 boost
- Group 3: chimera 4 prime/boost
- Group 4: SARS-CoV-2 spike furin KO prime/boost
- Group 5: Norovirus capsid prime/boost

Figure S7

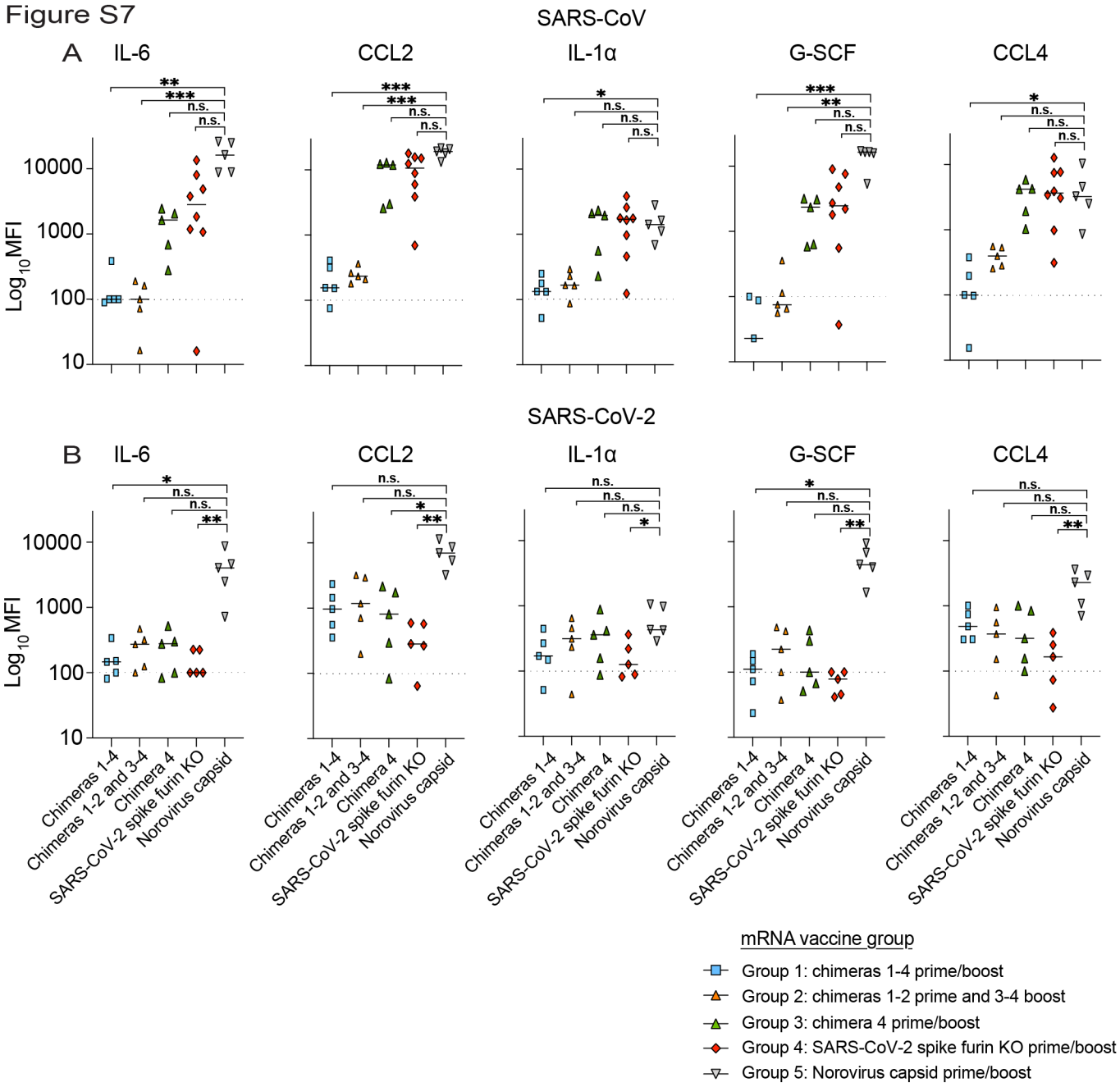

Table S1: Amino acid sequences of chimeric spikes

Chimera 1:	MFVFLVLLPLVSSQCGIISRKPQPKMAQVSSSRRGVYYNDDIFRSDVLHLTQDYFLPFDSNLTQYFSLNVDSDRYTYFD NPILDFGDGVYFAATEKSNVIRGWIFGSSFDNTTQSAVIVNNSTHIIIRVCNFNLCKEPMYTVSRGTQQNAWVYQSAFN CTYDRVEKSFQLDTTPKTGNFKDLREYVFKNRDGFLSVYQTYTAVNLPRGLPTGFSVLKPILKLPFGINITSYRVVMA MFSQTTSNFLPESAAYYVGNLKYSTFMLRFNENGTITDAVDCSQNPLAELKCTIKNFTVEKGIYQTSNFRVQPTESIVR FPNITNLCPFGEVFNATKFPSVYAWERKKISNCVADYSVLYNSTFFSTFKCYGVSATKLNDLCFSNVYADSFVVKGDD VRQIAPGQTGVIADYNYKLPDDFMGCVLAWNTRNIDATSTGNYNYKYRYLRHGKLRPFERDISNVPFSPDGKPCTPPA LNCYWPLNDYGFYTTTGIGYQPYRVVVLSFELLNAPATVCGPKKSTNLVKNKCVNFNFNGLTGTGVLTESNKKFLPF QQFGRDIADTTDAVRDPQTLEILDITPCSFGGVSVITPGTNTSNQVAVLYQDVNCTEVPVAIHADQLTPTWRVYSTGSN VFQTRAGCLIGAEHVNNSYECDIPIGAGICASYQTQTNSPRRARSVASQSIIAYTMSLGAENSVAYSNNSIAIPTNFTISV TTEILPVSMTKTSVDCTMYICGDSTECSNLLLQYGSFCTQLNRALTGIAVEQDKNTQEVFAQVKQIYKTPPIKDFGGFN FSQILPDPSKPSKRSFIEDLLFNKVTLADAGFIKQYGDCLGDIAARDLICAQKFNGLTVLPPLLTDEMIAQYTSALLAGT ITSGWTFGAGAALQIPFAMQMAYRFNGIGVTQNVLYENQKLIANQFNSAIGKIQDSLSSTASALGKLQDVVNQNAQAL NTLVKQLSSNFGAISSVLNDILSRLDKVEAEVQIDRLITGRLQSLQTYVTQQLIRAAEIRASANLAATKMSECVLGQSK RVDFCGKGYHLMSFPQSAPHGVVFLHVTYVPAQEKNFTTAPAICHDGKAHFPREGVFVSNGTHWFVTQRNFYEPQIIT TDNTFVSGNCDVVIGIVNNTVYDPLQPELDSFKEELDKYFKNHTSPDVDLGDISGINASVVNIQKEIDRLNEVAKNLNE SLIDLQELGKYEQYIKWPWYIWLGFIAGLIAIVMVTIMLCCMTSCCSCLKGCCSCGSCCKFDEDDSEPVLKGVKLHYT
Chimera 2:	MFIFLLFLTLTSGSDLDRCTTFDDVQAPNYTQHTSSMRGVYYPDEIFRSDTLYLTQDLFLPFYSNVTGFHTINHTFGNP VIPFKDGIYFAATEKSNVVRGWVFGSTMNNKSQSVIIINNSTNVVIRACNFELCDNPFFAVSKPMGTQTHTMIFDNAFN CTFEYISDAFSLDVSEKSGNFKHLREFVFKNKDGFLYVYKGYQPIDVVRDLPSGFNTLKPIFKLPLGINITNFRAILTAFS PAQDIWGTSAAAYFVGYLKPTTFMLKYDENGTITDAVDCSQNPLAELKCSVKSFEIDKGIYQTSNFRVVPSGDVVRFP NITNLCPFGEVFNATRFASVYAWNRKRISNCVADYSVLYNSASFSTFKCYGVSPTKLNDLCFTNVYADSFVIRGDEVR QIAPGQTGKIADYNYKLPDDFTGCVIAWNSNNLDSKVGGNYNYLYRLFRKSNLKPFERDISTEIYQAGSTPCNGVEGF NCYFPLQSYGFQPTNGVGYQPYRVVVLSFELLHAPATVCGPKLSTDLIKNQCVNFNFNGLTGTGVLTPSSKRFQPFQQ FGRDVSDFTDSVRDPKTSEILDISPCSFGGVSVITPGTNASSEVAVLYQDVNCTDVSTAIHADQLTPAWRIYSTGNNVF QTQAGCLIGAEHVDTSYECDIPIGAGICASYHTVSLLRSTSQKSIVAYTMSLGADSSIAYSNNTIAIPTNFSISITTEVMPV SMAKTSVDCNMYICGDSTECANLLLQYGSFCTQLNRALSGIAAEQDRNTREVFAQVKQMYKTPTLKYFGGFNFSQILP DPLKPTKRSFIEDLLFNKVTLADAGFMKQYGECLGDINARDLICAQKFNGLTVLPPLLTDDMIAAYTAALVSGTATAG WTFGAGAALQIPFAMQMAYRFNGIGVTQNVLYENQKQIANQFNKAISQIQESLTTTSTALGKLQDVVNQNAQALNTL VKQLSSNFGAISSVLNDILSRLDKVEAEVQIDRLITGRLQSLQTYVTQQLIRAAEIRASANLAATKMSECVLGQSKRVD FCGKGYHLMSFPQAAPHGVVFLHVTYVPSQERNFTTAPAICHEGKAYFPREGVFVFNGTSWFITQRNFFSPQIITTDNT FVSGNCDVVIGIINNTVYDPLQPELDSFKEELDKYFKNHTSPDVDLGDISGINASVVNIQKEIDRLNEVAKNLNESLIDL QELGKYEQYIKWPWYVWLGFIAGLIAIVMVTILLCCMTSCCSCLKGACSCGSCCKFDEDDSEPVLKGVKLHYT
Chimera 3:	MFVFLVLLPLVSSQCVNLTTRTQLPPAYTNSFTRGVYYPDKVFRSSVLHSTQDLFLPFFSNVTWFHAIHVSGTNGTKR FDNPVLPFNDGVYFASTEKSNIIRGWIFGTTLDSKTQSLLIVNNATNVVIKVCEFQFCNDPFLGVYYHKNNKSWMESEF RVYSSANNCTFEYVSQPFLMDLEGKQGNFKNLREFVFKNIDGYFKIYSKHTPINLVRDLPQGFSALEPLVDLPIGINITR FQTLLALHRSYLTPGDSSSGWTAGAAAYYVGYLQPRTFLLKYNENGTITDAVDCALDPLSETKCTLKSFTVEKGIYQT SNFRVQPTESIVRFPNITNLCPFGEVFNATKFPSVYAWERKKISNCVADYSVLYNSTFFSTFKCYGVSATKLNDLCFSN VYADSFVVKGDDVRQIAPGQTGVIADYNYKLPDDFMGCVLAWNTRNIDATSTGNYNYKYRYLRHGKLRPFERDISNV PFSPDGKPCTPPALNCYWPLNDYGFYTTTGIGYQPYRVVVLSFELLNAPATVCGPKKSTNLVKNKCVNFNFNGLTGT GVLTESNKKFLPFQQFGRDIADTTDAVRDPQTLEILDITPCSFGGVSVITPGTNTSNQVAVLYQDVNCTEVPVAIHADQ LTPTWRVYSTGSNVFQTRAGCLIGAEHVNNSYECDIPIGAGICASYQTQTNSPRRARSVASQSIIAYTMSLGAENSVAY SNNSIAIPTNFTISVTTEILPVSMTKTSVDCTMYICGDSTECSNLLLQYGSFCTQLNRALTGIAVEQDKNTQEVFAQVKQ IYKTPPIKDFGGFNFSQILPDPSKPSKRSFIEDLLFNKVTLADAGFIKQYGDCLGDIAARDLICAQKFNGLTVLPPLLTDE MIAQYTSALLAGTITSGWTFGAGAALQIPFAMQMAYRFNGIGVTQNVLYENQKLIANQFNSAIGKIQDSLSSTASALG KLQDVVNQNAQALNTLVKQLSSNFGAISSVLNDILSRLDKVEAEVQIDRLITGRLQSLQTYVTQQLIRAAEIRASANLA ATKMSECVLGQSKRVDFCGKGYHLMSFPQSAPHGVVFLHVTYVPAQEKNFTTAPAICHDGKAHFPREGVFVSNGTH WFVTQRNFYEPQIITTDNTFVSGNCDVVIGIVNNTVYDPLQPELDSFKEELDKYFKNHTSPDVDLGDISGINASVVNIQ KEIDRLNEVAKNLNESLIDLQELGKYEQYIKWPWYIWLGFIAGLIAIVMVTIMLCCMTSCCSCLKGCCSCGSCCKFDED DSEPVLKGVKLHYT
Chimera 4:	MFVFLVLLPLVSSQCVNLTTRTQLPPAYTNSFTRGVYYPDKVFRSSVLHSTQDLFLPFFSNVTWFHAIHVSGTNGTKR FDNPVLPFNDGVYFASTEKSNIIRGWIFGTTLDSKTQSLLIVNNATNVVIKVCEFQFCNDPFLGVYYHKNNKSWMESEF RVYSSANNCTFEYVSQPFLMDLEGKQGNFKNLREFVFKNIDGYFKIYSKHTPINLVRDLPQGFSALEPLVDLPIGINITR FQTLLALHRSYLTPGDSSSGWTAGAAAYYVGYLQPRTFLLKYNENGTITDAVDCALDPLSETKCTLKSFTVEKGIYQT SNFRVQPTESIVRFPNITNLCPFGEVFNATTFPSVYAWERKRISNCVADYSVLYNSTSFSTFKCYGVSATKLNDLCFSNV YADSFVVKGDDVRQIAPGQTGVIADYNYKLPDDFLGCVLAWNTNSKDSSTSGNYNYLYRWVRRSKLNPYERDLSNDI YSPGGQSCSAVGPNCYNPLRPYGFFTTAGVGHQPYRVVVLSFELLNAPATVCGPKKSTNLVKNKCVNFNFNGLTGTG VLTESNKKFLPFQQFGRDIADTTDAVRDPQTLEILDITPCSFGGVSVITPGTNTSNQVAVLYQDVNCTEVPVAIHADQL TPTWRVYSTGSNVFQTRAGCLIGAEHVNNSYECDIPIGAGICASYQTQTNSPRRARSVASQSIIAYTMSLGAENSVAYS NNSIAIPTNFTISVTTEILPVSMTKTSVDCTMYICGDSTECSNLLLQYGSFCTQLNRALTGIAVEQDKNTQEVFAQVKQI YKTPPIKDFGGFNFSQILPDPSKPSKRSFIEDLLFNKVTLADAGFIKQYGDCLGDIAARDLICAQKFNGLTVLPPLLTDE MIAQYTSALLAGTITSGWTFGAGAALQIPFAMQMAYRFNGIGVTQNVLYENQKLIANQFNSAIGKIQDSLSSTASALG KLQDVVNQNAQALNTLVKQLSSNFGAISSVLNDILSRLDKVEAEVQIDRLITGRLQSLQTYVTQQLIRAAEIRASANLA ATKMSECVLGQSKRVDFCGKGYHLMSFPQSAPHGVVFLHVTYVPAQEKNFTTAPAICHDGKAHFPREGVFVSNGTH WFVTQRNFYEPQIITTDNTFVSGNCDVVIGIVNNTVYDPLQPELDSFKEELDKYFKNHTSPDVDLGDISGINASVVNIQ KEIDRLNEVAKNLNESLIDLQELGKYEQYIKWPWYIWLGFIAGLIAIVMVTIMLCCMTSCCSCLKGCCSCGSCCKFDED DSEPVLKGVKLHYT